Geminga's pulsar halo: a multiwavelength view

Silvia Manconi [1,2] *Jooyun Woo* [1,3] *Ruo-Yu Shang* [1,4] Roman Krivonos [5] Claudia Tang [4] Mattia Di Mauro [6] Fiorenza Donato [6,7] *Kaya Mori* [1,3]
Charles J. Hailey [3]

[1]*in presence at the Symposium!* [2]*LAPTh, CNRS (FR)* [3]*Columbia Astrophysics Lab (USA)* [4]*Department of Physics and Astronomy, Columbia University (USA)* [5]*IKI (RF)* [6]*INFN Turin (IT)* [7]*University of Turin (IT)*

In short

We present [1] a broadband investigation of the Geminga pulsar halo using novel X-ray analysis of archival data, existing γ-ray observations and state-of-the-art phenomenological models, finding constraints to the magnetic field strength around Geminga.

A multiwavelength halo around Geminga?

Pulsar halos are emerging as a general characteristic of middle-aged (few 100 kyrs old) Galactic pulsars: non-thermal γ-rays extending at least a few tens of parsec around energetic pulsars, and well beyond boundaries of pulsar wind nebulae observed in radio and X-ray bands

Geminga is the first pulsar around which a remarkable gamma-ray halo extending over a few degrees was discovered at TeV by MILAGRO, HAWC and later by H.E.S.S., and by Fermi-LAT at GeV energies [2, 3, 4]

Origin: energetic $e^{\pm}$ accelerated by the pulsar and producing inverse Compton scattering emission off the ambient radiation fields after escaping the relic pulsar wind nebula

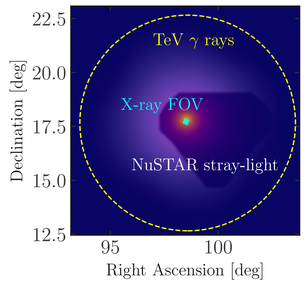

Figure 1. Geminga synchrotron halo flux for 8–40 keV, overlaid with the extension of TeV γ rays (yellow), and typical X-ray field of view (FOV) for focused (cyan) and stray-light (unshaded) photon components.

If emission at ∼GeV-TeV originate from high energy $e^{\pm}$, synchrotron losses in ambient magnetic field produce *diffuse synchrotron emission with similar spatial extension* at X-ray energies, providing constraints to the magnetic field strength and to $e^{\pm}$ properties (cutoff, injection)

Challenges: theoretical understanding of inferred properties in the vicinity of pulsars, crucial for interpreting cosmic-ray positron excess and for Galactic cosmic ray propagation

Synchrotron halo: γ ray-informed modelling

Observed halo's spectral and morphological properties suggest that $e^{\pm}$ *diffusion is suppressed* with respect to what found to average describe Galactic cosmic ray propagation

We use a phenomenological model explaining Fermi-LAT, HAWC and H.E.S.S. data [4]:

⋆ $e^{\pm}$ emitted by the pulsar $\mathcal{N}_e$ propagated with (inhibited) diffusion-loss equation, $D(E) \propto D_0 E^{-\delta}$

$$\frac{\partial \mathcal{N}_e}{\partial t} - \nabla \cdot \{D(E)\nabla \mathcal{N}_e\} + \frac{\partial}{\partial E}\left\{\frac{dE}{dt}\mathcal{N}_e\right\} = Q(E, \mathbf{x}, t)$$

⋆ Synchrotron and inverse Compton emission (spectrum, angular profile, 2D template):

$$\Phi_\gamma(E_\gamma, \Delta\Omega) = \frac{1}{4\pi}\int_{m_e c^2}^{\infty} dE \int_{\Delta\Omega} d\Omega \int_0^{\infty} ds\, \mathcal{N}_e(E, s, t)\mathcal{P}_{\rm IC,synch}(E, E_\gamma)$$

Similarly to what predicted for γ rays, for very low D_0 the X-ray halo is highly concentrated towards the inner ∼1 degree, while higher values distribute the emission over larger angular scales, making a significant X-ray detection challenging

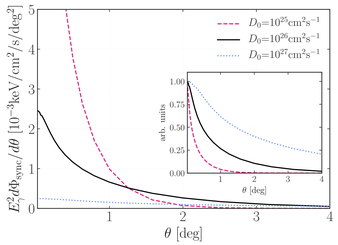

Figure 2: Effect of the diffusion coefficient D_0 on the Geminga's halo angular profile for [10–40] keV. The inset shows the flux profile normalised at $\theta = 0$, in arbitrary units.

X-ray data: upper limits with XMM-Newton and NuSTAR

We analyse archival X-ray data in a *broad energy range* (XMM–Newton: + NuSTAR: 8-79 keV). Since Geminga halo is expected to be extended as the FOV of both instruments, we developed *innovative techniques* carefully estimating the backgrounds

No detection: robust upper bounds on the X-ray diffuse emission from the Geminga halo

XMM-Newton
0.5 - 8 keV, two bins
FOV: 900" radius around pulsar

Novel approach: Individual background components derived using control regions, in which background events are dominant, allowing the measurement of the absolute level of Geminga halo emission in the signal region independent of the control regions

Energy spectrum + angular profile constraints

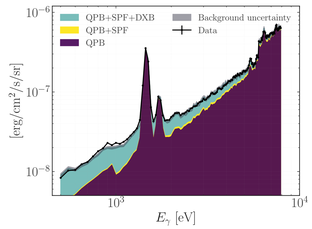

Figure 3. X-ray spectrum in [0.5, 8] keV range in XMM–Newton data. The data (black) is overlaid with the expected background components, including quiescent particle background (QPB, purple), soft-proton flare (SPF, yellow), and diffuse X-ray background (DXB, green). The grey band shows the size of background uncertainty, used to estimate upper limits.

NuSTAR
8-79 keV, two bins
Novel technique considering both focused and stray-light X-ray components for spatially non-uniform diffuse X-ray emission

Focused photons: background region for background estimation
Stray-light: simulation (see next)

Observation for background estimation: similar pointing angle (left)

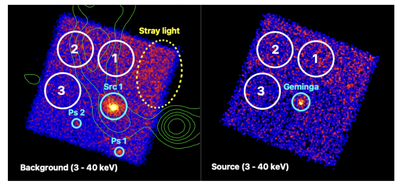

Figure 4. NuSTAR Background and source counts maps for the energy bin 3-40 keV. Our regions of interest (region 1–3) are marked with white circles. Detected sources (Src 1, Ps 1 and 2, Geminga) are marked with cyan circles. Local stray light background only present in the background observation is marked with yellow dashed ellipse. VLA 74 MHz contour of IC 443 is overlaid in green.

NuSTAR: X-ray halo model convolution

No X-ray halo detection with NuSTAR: upper limits on the flux are derived using the observed count rates, and the physical Geminga synchrotron halo model, which is non-uniform in the region

To simulate realistic count rates, the model surface brightness is separately convoluted with:

- the optics (2-bounce photons), using `SIXTE`
- the collimator response functions (stray-light photons), using `NUSKYBGD`

and then combined in each of the three circular regions defined in Figure 4.

The stray-light background component is found to be as significant as the focused halo component, and dominant over the focused halo component in the 40-79 keV energy band

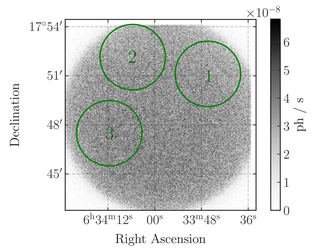

Figure 5. Count rate from the SIXTE simulation of the Geminga halo corresponding to the derived upper limits in 8-40 keV. The three circular regions used to extract the count rates to compare with the background subtracted data are also shown in green. The simulated exposure is 10^9 s, to ensure statistical errors are negligible

Interpretation of multiwavelength spectral energy distribution

Model for inverse Compton integrated in 30, 10, 1 degrees; synchrotron in 0.23 degrees (∼FOV)

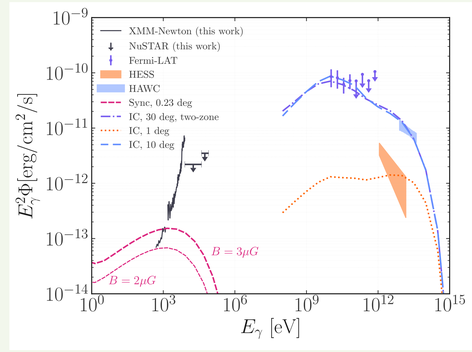

Figure 6. Interpretation of all available Geminga pulsar halo data, from gamma rays (Fermi-LAT, H.E.S.S., HAWC) to the X-ray upper limits (XMM–Newton, NuSTAR). The inverse Compton and synchrotron emissions are obtained within a model in which $e^{\pm}$ pairs diffuse in a low diffusion zone.

- XMM-Newton constrain: B to be less than 2μG, compatible with eRosita [5] and independent local B estimates [6]; $D0 > 6 \cdot 10^{25}$/cm^2/s
- NuSTAR less constraining at few keV, but > 10 keV are crucial to constrain energy cutoff
- Angular profile upper limits: less constraining

Full parameter space investigation left to future work.

Summary

XMM	New data analysis optimized to search for extended objects exceeding field of view; robust and constraining upper limits to intensity and spatial profile
NuSTAR	Energies larger than 10 keV explored for the first time, demonstrating importance of stray-light when analysing sources extending few degrees
Model	Interpretation of all current broadband observation of Geminga halo, from X-ray to multi-TeV gamma-rays within phenomenological model taking into account suppressed diffusion, inverse Compton and synchrotron energy losses of accelerated $e^{\pm}$
Result	XMM observations at few keV constrain magnetic field around Geminga to be less than 2μG
Outlook	Methodology can be applied to other pulsar halos with archived data or future observations

SM acknowledges the European Union's Horizon Europe research and innovation program for support under the Marie Sklodowska-Curie Action HE MSCA PF–2021, grant agreement No.10106280, project VerSi.

References

See full bibliography in [1] for more references, in particular on the theoretical modelling.

[1] S. Manconi, J. Woo, R.-Y. Shang, R. Krivonos, C. Tang, M. Di Mauro, F. Donato, K. Mori, and C. J. Hailey *to appear in* A&A, 2024.
[2] A. U. Abeysekara *et al. Science*, vol. 358, no. 6365, pp. 911–914, 2017.
[3] F. Aharonian *et al. Astron. Astrophys.*, vol. 673, p. A148, 2023.
[4] M. Di Mauro, S. Manconi, and F. Donato *Phys. Rev. D*, vol. 100, no. 12, p. 123015, 2019.
[5] A. Khokhriakova, W. Becker, G. Ponti, M. Sasaki, B. Li, and R. Y. Liu *Astron. Astrophys.*, vol. 683, p. A180, 2024.
[6] R. Jansson and G. R. Farrar , vol. 761, p. L11, Dec. 2012.
[7] R.-Y. Liu, C. Ge, X.-N. Sun, and X.-Y. Wang *Astrophys. J.*, vol. 875, no. 2, p. 149, 2019.